

and F. Whitby for assistance with data collection; V. Ramakrishnan and members of the Sundquist and Hill laboratories for critical comments on the manuscript; M. Martin for plasmid pNL4-3; D. Trono for plasmid R9; and J. Cassatt for support and encouragement. Supported by NIH grants RO1 AI40333 and RO1 AI43036 (W.I.S. and C.P.H.), the Lucille P.

Markey Charitable Trust, and a postdoctoral fellowship from the Cancer Research Institute (T.R.G.). Coordinates (1am3) and diffraction data (r1am3sf) for CA(151–231) have been deposited in the Protein Data Bank (Brookhaven National Laboratory).

17 March 1997; accepted 23 September 1997

Metal Ion Chaperone Function of the Soluble Cu(I) Receptor Atx1

R. A. Pufahl, C. P. Singer, K. L. Peariso, S.-J. Lin,
P. J. Schmidt, C. J. Fahrni, V. Cizewski Culotta,
J. E. Penner-Hahn, T. V. O'Halloran*

Reactive and potentially toxic cofactors such as copper ions are imported into eukaryotic cells and incorporated into target proteins by unknown mechanisms. Atx1, a prototypical copper chaperone protein from yeast, has now been shown to act as a soluble cytoplasmic copper(I) receptor that can adopt either a two- or three-coordinate metal center in the active site. Atx1 also associated directly with the Atx1-like cytosolic domains of Ccc2, a vesicular protein defined in genetic studies as a member of the copper-trafficking pathway. The unusual structure and dynamics of Atx1 suggest a copper exchange function for this protein and related domains in the Menkes and Wilson disease proteins.

Although Cu is an essential cofactor for mitochondrial, cytosolic, and vesicular oxygen-processing enzymes (1), it can be toxic even at low concentrations. Cu(I) and Cu(II) ions can bind with high affinity to adventitious sites in partially folded proteins and catalyze auto-oxidation of lipids, proteins, and nucleic acids. To investigate the mechanisms by which cells overcome the dilemma of maintaining Cu availability while controlling deleterious reactivity of the free ions, we have determined the Cu chemistry and Cu-handling function of Atx1, an intracellular eukaryotic protein implicated in Cu trafficking. Our results indicate that Atx1 functions as a metal ion chaperone, a protein that protects and guides Cu(I) ions to activate target enzymes.

ATX1 is one of several genes in the Cu-dependent, high-affinity iron uptake pathway in yeast. These genes encode Ctr1, a Cu uptake protein in the plasma membrane; Ccc2, an intracellular membrane protein; and the multicopper oxidase Fet3 (2–6). Although the role of Fet3 in iron uptake is unclear, Cu loading into this enzyme occurs in a post-

Golgi vesicle and is mediated by Ccc2 (4). The ATX1 gene and its human homolog, HAH1, encode cytosolic proteins implicated in Cu trafficking to these Ccc2-containing vesicles (7–9). The Ccc2 protein in yeast and its human homologs, the Menkes disease protein (10) and Wilson disease protein (11), are members of the P-type adenosine triphosphatase (ATPase) cation transporter family (12) and are present in the membranes of secretory vesicles (13). Each transporter contains two or more Atx1-like cytoplasmic domains (Fig. 1), the functions of which are not known. The conserved MTCXXC sequence (X, any residue), a motif observed in several bacterial Hg(II) transport proteins (14), is thought to be a Cu binding site, although it does not correspond to known Cu(I) or Cu(II) sites in structurally characterized proteins. Establishing the Cu oxidation state and coordination environment in Atx1 should provide insight into its function and that of the homologous domains in its partner proteins.

Atx1 was expressed in *Escherichia coli* and purified as the apoprotein (15). Addition of CuSO₄ to apo-Atx1 in the presence of excess thiol reproducibly yielded a complex with a copper/protein ratio of 0.6 to 0.8 (16). Gel filtration experiments indicated that the predominant form of the protein was a monomer under these conditions, regardless of the presence or absence of Cu (15). The Cu oxidation state was investigated by electron paramagnetic resonance (EPR) spectroscopy and x-ray absorption spectroscopy (XAS). No EPR signal was observed at 77 K, suggesting the ab-

sence of a mononuclear Cu(II) site. XAS experiments (17) indicated that the bulk sample contained Cu(I). The Cu-Atx1 x-ray absorption near edge structure (XANES) spectrum exhibited a weak shoulder at 8984 eV, which is typical of Cu(I) and inconsistent with comparable edge features for Cu(II) compounds, the energies of which are 3 to 4 eV greater (Fig. 2A). The intensity of the 8984-eV transition varies with Cu(I) geometry, ranging from low for tetrahedral sites to high and well resolved for digonal sites (18). The observed transition is typical of those of trigonal Cu(I) model compounds (Fig. 2A). Mononuclear Cu(I) coordination complexes, however, are usually not stable in aqueous solution, and typically undergo auto-oxidation or disproportionation reactions to give Cu(II) (aqueous) and Cu(solid). In contrast, millimolar concentrations of Cu(I)-Atx1 are stable in air at neutral pH for at least 30 min (16), suggesting that the coordination environment in Atx1 stabilizes the Cu(I) state and suppresses disproportionation.

Proteins that stabilize Cu(I) form either polynuclear metal thiolate clusters, as in metallothionein and the transcription factors Ace1, CUP2, and AMT (19), or a constrained His₂Cys coordination environment, as in blue copper proteins (20). In contrast, extended x-ray absorption fine structure (EXAFS) measurements indicated that Atx1 stabilization of Cu(I) is achieved in a mononuclear site through an all-sulfur coordination environment (Fig. 2B). The high intensity and relatively high frequency of the EXAFS oscillations were typical of those observed for Cu-S interactions. The data could be modeled with a single three-sulfur (3S) shell with a Cu-S distance of 2.26 Å; however, the Debye-Waller factor, σ^2 , was somewhat larger than expected ($7 \times 10^{-3} \text{ \AA}^2$). This Cu-S distance is typical of three-coordinate Cu (21–23) and is 0.1 Å longer than that in two-coordinate Cu-thiolate complexes (24). Given that Atx1 contains only two conserved cysteine residues, the third ligand can be either a low-Z (atomic number) ligand (O or N), a methionine sulfur, or an exogenous thiol. A 2S + 1S fit with a shell of two sulfurs at 2.25 Å and a shell of one sulfur at 2.40 Å reproduced the data better than did the single-shell fit, and gave more reasonable σ^2 values (3×10^{-3} and 5×10^{-3} to $6 \times 10^{-3} \text{ \AA}^2$, respectively). Furthermore, attempts to model the data with a shell of 2S and a low-Z shell (1N) gave chemically unrealistic Debye-Waller factors for the N shell ($\sigma^2 \leq 0$).

The 2S + 1S result is unexpected for several reasons. The most common coordination environment for Cu(I) complexes is distorted four-coordinate, and there are few precedents among mononuclear Cu(I) complexes for the low-coordination number environ-

R. A. Pufahl, C. P. Singer, C. J. Fahrni, T. V. O'Halloran, Department of Chemistry and Department of Biochemistry, Molecular Biology, and Cell Biology, Northwestern University, Evanston, IL 60208, USA.

K. L. Peariso and J. E. Penner-Hahn, Department of Chemistry, University of Michigan, Ann Arbor, MI 48109, USA.

S.-J. Lin, P. J. Schmidt, V. Cizewski Culotta, Department of Environmental Health Sciences, Johns Hopkins University, Baltimore, MD 21205, USA.

*To whom correspondence should be addressed. E-mail: t-ohalloran@nwu.edu

Fig. 1. Homology among MXCXC-containing proteins. Identical regions are shaded dark and regions displaying high homology are light. Areas with internal gaps are indicated by a period. Proteins (with accession number) are as follows: Atx1, *Saccharomyces cerevisiae* (L35270); Hah1, *Homo sapiens* (U70660); Ccc2, *S. cerevisiae* (L36317); Wilson disease protein, *H. sapiens* (U11700); Menkes disease protein, *H. sapiens* (L06133); MerP, *Pseudomonas aeruginosa* (Z00027). Partial amino acid sequences of some proteins are as follows: Ccc2-d1, amino acids 1 to 71, Ccc2-d2, amino acids 76 to 150, Wilson1, amino acids 54 to 125, Menkes1, amino acids 4 to 75, and MerP, 20 to 91. The figure was created with the Pileup program from the Wisconsin Package, Version 9.0, from the Genetics Computer Group (GCG). Abbreviations for the amino acid residues are as follows: A, Ala; C, Cys; D, Asp; E, Glu; F, Phe; G, Gly; H, His; I, Ile; K, Lys; L, Leu; M, Met; N, Asn; P, Pro; Q, Gln; R, Arg; S, Ser; T, Thr; V, Val; W, Trp; and Y, Tyr.

Atx1	MAEIKHYQF	NVV.MTCGSC	SGAVNKVLTK	LEPDVSKIDH	SLEKQLVDVY	TTLPYDFILE	KIKKTGKEVR	.SGKQL
Hah1	MPKHEF	SVD.MTCGGC	AEAVSRVLNK	L.GGVKDYD	DLPNKKVCIE	SEHSMDLLA	TLKKTGKTVS	TLGLE
Ccc2-d1	MREVIL	AVHGMTCSAC	TNTINTQLRA	LK.GVTKCDI	SLVTNECQVT	VD.NEVTADS	IKKIEHDCGF	DCEILRD
Ccc2-d2	AISTKEGLL	SVQCMTCGSC	VSTVTKQVEG	IE.GVESVYV	SLVTEECHVI	YEPSKTHLET	AREMIEDCGF	DSNIIMD
Wilson1	SSQVATSTV	RIIGMTCQSC	VKSIEDRISN	LK.GHISMKV	SLEQGSATVK	YVPSVVCLOQ	VCHQIGDMGF	EAST
Menkes1	SMGVNSVTI	SVEGMTCSNC	VYVTEQQIGK	VN.GVHHIKV	SLEEKNTATII	YDPKLOPKPT	LQEAIDDMGF	DAVI
MerP	ATQTVTL	SVPGMTCGSC	PITVKKALSE	VE.GVSKVDV	EEETROAVVT	EDDAKTSVQK	LTKATADAGY	PSSVKQ

ment in Atx1 (23, 24). Furthermore, no other native Cu-proteins are known to coordinate a mononuclear Cu center through two cysteines, regardless of the absence or presence of other ligands.

XAS and multinuclear nuclear magnetic resonance (NMR) spectroscopy revealed that the protein conformation does not impose a rigid three-coordinate geometry on the metal ion: Atx1 will also accommodate lower coordination numbers. In these experiments, we used Hg(II), a metal ion with a d^{10} electronic configuration that exhibits several similarities to Cu(I). The results were consistent with Hg(II) coordination by two Cys thiolates in Hg-Atx1. A ^{199}Hg single broad resonance was observed at -821 parts per million (ppm) for Hg-Atx1 (Fig. 3) (25). This chemical shift is consistent with either a linear dithiolate arrangement, which typically exhibits resonances from -790 to -1000 ppm (26), or a blue copper environment (type I site), consisting of two His, one Met, and one Cys, which have chemical shifts that range from -700 to -890 ppm (27, 28). Given that Atx1 contains only one His, a canonical type I site is not possible. The dithiolate coordination environment for Hg-Atx1 is supported by three additional lines of reasoning: (i) $^1\text{H}\{^{199}\text{Hg}\}$ heteronuclear multiple-quantum coherence (HMQC) spectra of Hg-Atx1 revealed coupling only to the Cys β -methylene protons. No coupling was observed for either Met or His protons (29). (ii) The line width in Hg-Atx1 was greater than that observed for Hg-substituted blue copper proteins, which is consistent with a center of lower symmetry. And (iii), EXAFS data for Hg-Atx1 exhibited a single peak that was well modeled by a single shell of two sulfurs at 2.34 Å. Fits with a higher coordination number were poor. Thus, the Hg-S bond lengths, refined coordination number, and chemical shift are typical of two-coordinate mercury thiolate centers in model compounds and Hg-peptides (30). On the basis of the ready accessibility of the two-coordinate state, the similarities between Cu(I) and Hg(II), and coordination chemistry principles delineated below, rapid rates of metal ion transfer from Atx1 to a Cu acceptor protein such as Ccc2 are anticipated.

Atx1 binds Cu(I) even in the presence of a 20-fold excess of competing thiols (16). This high-affinity Cu binding is consistent with hard-soft acid-base principles and the chelate effect. The strength of the chemical bonds between the soft sulfur atoms and highly polarizable d^{10} centers such as Cu(I) and Hg(II) is typically so great that it is difficult to measure, which has led to the belief that Cu(I) exchange out of proteins with thiolate-rich coordination sites must be slow (31). In instances in which the metal center can adopt a low coordination number and an incoming ligand forms a bond of similar strength to those of the other metal ligands, however, a

facile associative mechanism can operate. A three-coordinate intermediate forms that can subsequently lose one of the original ligands to give a new two-coordinate center. When all three metal-ligand bonds are of similar bond energy, rapid ligand exchange is typically observed. An example of thermodynamically tight binding with a rapid rate of ligand exchange is provided by the chemistry of Hg(II) thiolate complexes; the formation constant for $\text{Hg}(\text{SR})_2$ is 10^{40} and the rate of thiol exchange is almost diffusion controlled (26, 32).

To test this direct Cu transfer mechanism, we used two hybrid experiments with Atx1 and Ccc2. The entire 73-amino acid coding region of Atx1 was fused in frame to that of the DNA-binding domain of Gal4, whereas the coding region for the Gal4 activation domain was fused to those for a series of segments of the Ccc2 polypeptide (33). Ccc2 is predicted to possess four cytoplasmic domains interspersed by eight membrane-spanning domains (5). The most NH_2 -terminal of these cytoplasmic domains (Ccc2-a) contains two MTCXXC Cu-binding motifs (5). Enhanced β -galactosidase (β -Gal) activity was observed only in yeast cells expressing sepa-

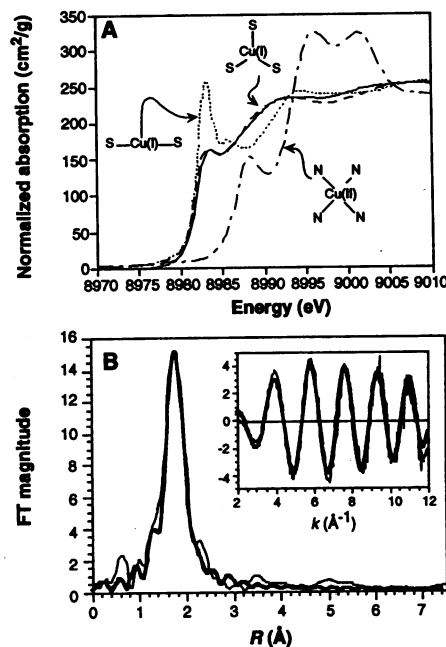


Fig. 2. Normalized Cu XANES (A) and EXAFS (B) spectra. (A) XANES spectra. Solid line, Cu-Atx1; dashed line, $[(\text{C}_6\text{H}_5)_4\text{P}]\text{Cu}(\text{SC}_6\text{H}_5)_3$ (23); dotted line, $[\text{N}(\text{C}_3\text{H}_7)_4]\text{Cu}(\text{SC}_{10}\text{H}_{13})_2$ (24); dashed-dotted line, $[\text{Cu}(\text{II})(\text{imidazole})_4](\text{NO}_3)_2$. (B) Fourier transform (FT) of k^3 weighted EXAFS data for Cu-Atx1, where R is the phase-shifted absorber-scatterer distance. (Inset) EXAFS data, where k is photoelectron wave vector. Thin lines represent data; thick lines are the best fit with two shells with $2S$ at 2.25 Å ($\sigma^2 = 3 \times 10^{-3}$ Å 2) and $1S$ at 2.40 Å ($\sigma^2 = 5 \times 10^{-3}$ to 6×10^{-3} Å 2).

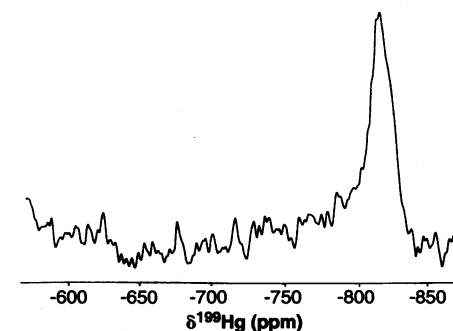
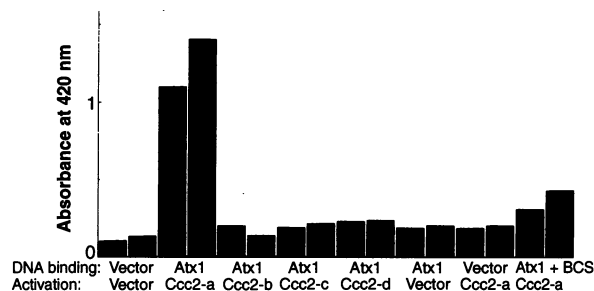


Fig. 3. NMR spectrum of a 2.4-mM solution of ^{199}Hg -Atx1. A single resonance at -821 ppm [relative to $\text{Hg}(\text{CH}_3)_2$] and a $\nu_{1/2}$ (line width at half peak height) of 2100 Hz were observed. Experiments were performed on a Bruker 600-MHz spectrometer with a 5-mm tunable broadband probe. The spectrum was collected at 20°C with 110,000 scans, a 90° pulse angle (determined to be 12.5 μs), a sweep width of 83,333 Hz, and a relaxation delay of 150 ms.

Fig. 4. Two-hybrid analysis of the interaction of Atx1 with Ccc2. Yeast strain SFY526 transformed with vectors based on pGBT9 (Gal4 DNA-binding domain) and pGAD424 (Gal4 activation domain) was subjected to measurements of β -Gal activity (absorbance at 420 nm). Where indicated, cells were grown in the presence of the Cu-chelator BCS. Data are shown for two independent transformants. Plasmids: Atx1, pPS002 (ATX1 in pGBT9); Ccc2-a, pPS001 (CCC2 DNA encoding amino acids 1 to 248 in pGAD424); Ccc2-b, pCF12 (CCC2 DNA encoding amino acids 388 to 527 in pGAD424); Ccc2-c, pCF34 (CCC2 DNA encoding amino acids 594 to 903 in pGAD424); Ccc2-d, pCF56 (CCC2 DNA encoding amino acids 994 to 1004 in pGAD424).



rate fusions of Atx1 and Ccc2-a (Fig. 4). These results indicate that Atx1 directly interacts with the NH₂-terminal region of Ccc2. The Cu-specific chelator bathocuproine disulfonic acid (BCS) inhibited β -Gal activity only in the strains expressing Ccc2-a and Atx1, indicating that the interaction of Atx1 with Ccc2 is dependent on Cu ions. These data are consistent with a Cu exchange mechanism in which Atx1 directly contacts the homologous domains in Ccc2 and donates Cu(I) through a metal-bridged intermediate.

On the basis of the Cu(I)-Atx1 coordination chemistry, the Cu-dependent interaction of Atx1 with Ccc2-a, and first principles, we propose a chemical exchange mechanism and one branch of the Cu-trafficking pathways in yeast (Fig. 5). After Cu import into the cell by Ctr1, Cu(I) binds to apo-Atx1 and the com-

plex diffuses throughout the cytoplasm. Cu(I) is coordinated to the two Cys residues of Atx1 and is weakly bound to a third sulfur atom. The latter could be from an adjacent Atx1 molecule, a buffer thiol, or a Met side chain. The Met (M13) can be mutated to Leu without loss of Atx1 activity in vivo, indicating that the latter possibility is unlikely. The distant third sulfur atom is predicted to be in rapid equilibrium between the bound and unbound state. On encountering its target, the Ccc2 molecule, Cu-Atx1 associates with the cytosolic Atx1-like domains. Such an association may be stabilized by a Cu-induced protein-protein interaction or through a Cu(I) bridge between Atx1 and Ccc2-a (or both). The Cu(I) then undergoes a series of rapid associative exchange reactions involving well-precedented

two- and three-coordinate intermediates, moving from Atx1 to Ccc2-a [Fig. 5 (inset)]. This mechanism provides an avenue for a diffusion-driven movement of the Cu(I) from one site in the cell to another on the basis of small differences in the binding constants of each domain for Cu(I). Such a flow is basically a vectorial process with the Cu(I) ion being directly and rapidly passed down a local thermodynamic gradient, from Cu(I) binding sites of lower affinity to higher affinity sites, without being released to the cytoplasm. If the free energy changes for each of these steps are coupled, hydrolysis of adenosine triphosphate by Ccc2 may provide the overall driving force by moving Cu(I) ions across the vesicular membrane into a separate compartment, where they are ultimately incorporated into Fet3.

By delivering essential cofactors or substrates to apoenzymes, the emerging class of metal ion chaperones facilitates formation of an active state of a protein. These chaperones guide metal ions to their appropriate biological partners and protect them from being trapped at adventitious sites. They may also protect cellular components by sequestering specific ions or inorganic clusters (34) and preventing adverse reactions. Our results underscore the idea that cells make use of elaborate machinery for recruiting, trafficking, compartmentalizing, and, ultimately, inserting into the appropriate enzyme reactive cofactors such as mononuclear Cu ions. The intracellular activation of apometalloenzymes by binding of the correct metal ion cofactors is unlikely to proceed by spontaneous self-assembly. Rather, metal insertion is emerging as an orchestrated event controlled by metal ion transport and chaperone proteins whose functions are kinetically and thermodynamically coupled.

Note added in proof: The three-dimensional structures of Hg-MerP (35) and MNK4 (36) have recently been determined by NMR methods. The MNK4 and MerP proteins exhibit the same protein fold, supporting the alignment in Fig. 1. The ¹⁹⁹Hg-NMR chemical shift of Hg-MerP (-816 ppm) corresponds to a linear S-Hg-S environment, further corroborating the assignment for Hg-Atx1. In addition, two other Cu chaperone proteins have been found in yeast and humans (37). Lys7 from *S. cerevisiae*, and Ccs from *H. sapiens* are required for incorporation of Cu into superoxide dismutase. Both proteins contain a single MXCXXC motif.

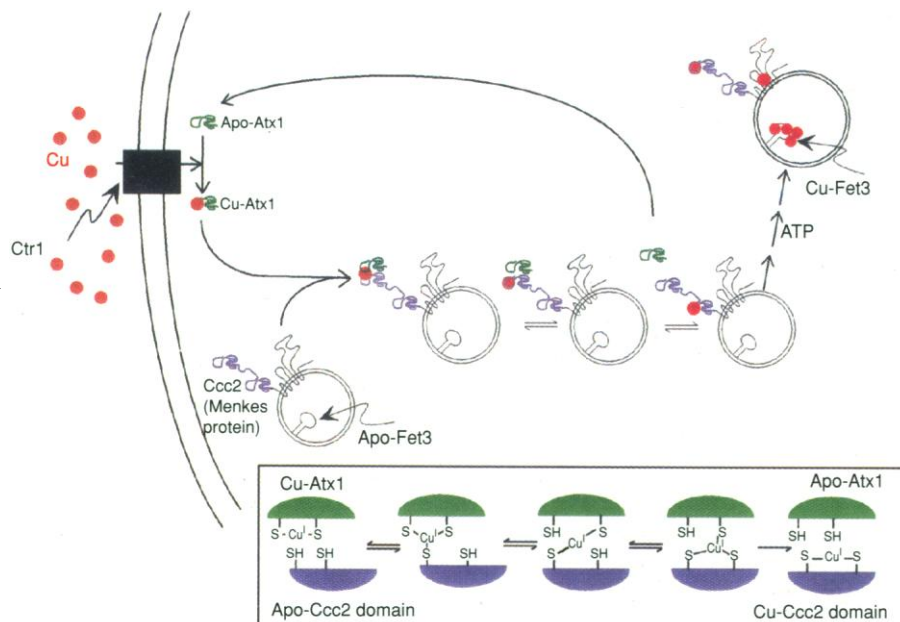


Fig. 5. Proposed path for the intracellular transfer of Cu(I) by Atx1. Copper destined for incorporation into the vesicular multicopper oxidase Fet3 requires both Ctr1 and Ccc2. Cytoplasmic Cu(I)-Atx1, but not apo-Atx1, associates with the NH₂-terminal domain of Ccc2 (purple) and Cu(I) is transferred to the latter. (Inset) A proposed mechanism for the exchange of Cu(I) involving two- and three-coordinate Cu-bridged intermediates. The human homologs of Atx1 (Hah1), Ccc2 (Menkes and Wilson proteins), and Fet3 (ceruloplasmin) are likely to employ similar mechanisms.

REFERENCES AND NOTES

1. J. S. Valentine, in *Bioinorganic Chemistry*, I. Bertini *et al.*, Eds. (University Science Books, Sausalito, CA, 1994), pp. 253-313.
2. C. Askwith *et al.*, *Cell* **76**, 403 (1994).
3. A. Dancis *et al.*, *J. Biol. Chem.* **269**, 25660 (1994).
4. R. Stearman *et al.*, *Science* **271**, 1552 (1996).
5. D. Fu *et al.*, *Yeast* **11**, 283 (1995).
6. D. S. Yuan *et al.*, *Proc. Natl. Acad. Sci. U.S.A.* **92**, 2632 (1995).

7. S.-J. Lin and V. Cizewski Culotta, *ibid.*, p. 3748.
8. S.-J. Lin, R. A. Pufahl, A. Dancis, T. V. O'Halloran, V. Cizewski Culotta, *J. Biol. Chem.* **272**, 9214 (1997).
9. L. W. J. Klomp *et al.*, *ibid.*, p. 9221.
10. C. Vulpe *et al.*, *Nature Genet.* **3**, 7 (1993).
11. P. C. Bull *et al.*, *ibid.* **5**, 327 (1993); R. E. Tanzi *et al.*, *ibid.*, p. 344.
12. S. Lutsenko and J. H. Kaplan, *Biochemistry* **34**, 15607 (1995).
13. M. J. Petris *et al.*, *EMBO J.* **15**, 6084 (1996).
14. P. C. Bull and D. W. Cox, *Trends Genet.* **10**, 246 (1994); P.-O. Eriksson and L. Sahlman, *J. Biomol. NMR* **3**, 613 (1993); J. L. Hobman and N. L. Brown, in *Metal Ions in Biological Systems*, A. Sigel and H. Sigel, Eds. (Decker, New York, 1997), vol. 34, pp. 527-568.
15. *ATX1* was cloned into pET11d (Novagen) and expressed in *E. coli* strain BL21(DE3) after induction with IPTG. The protein was isolated by a freeze-thaw extraction and purified to homogeneity by DEAE-Sephacel batch treatment and subsequent chromatography on CM Sepharose FF (Pharmacia). Approximately 6 to 10 mg of pure protein was obtained per liter of bacterial culture. Protein concentration was determined from absorbance at 280 nm (with an extinction coefficient of 4400 M⁻¹ cm⁻¹, calculated on the basis of total amino acid composition) or by Bradford assay [M. Bradford *Anal. Biochem.* **72**, 248 (1976)] with immunoglobulin G as a standard. Electrospray mass spectrometry (ES-MS) of apo-Atx1 revealed a single peak of 8088.1 daltons, which corresponds to full-length Atx1 lacking its NH₂-terminal methionine; in addition, ES-MS of Hg-Atx1 yielded one peak at 8287.6 daltons. Gel filtration on an HPLC QC-PAK TSK 200GL (TosoHaas) column yielded molecular sizes of 10,200, 9840, and 9960 daltons for apo-, Hg(II)-, and Cu(I)-Atx1, respectively.
16. Cu(I)-Atx1 was typically prepared by incubation of apo-Atx1 with a Cu(II) salt in the presence of a thiol reductant. All manipulations were performed in an inert atmosphere at 4°C. CuSO₄ (2.5 equivalents) was added, with stirring, to a solution of apo-Atx1 and DTT (20-fold molar excess relative to protein) in 50 mM Tris (pH 8.0, adjusted with solid MES to avoid Cl⁻). Excess metal was removed by ultrafiltration and the protein was exchanged into a solution containing 20 mM MES (pH 6.0) and 20% (v/v) glycerol. The final protein concentration was 7.84 mM with a Cu/protein ratio of 0.75 ± 0.02. Solutions (>2 mM) of the Cu(I)-protein can be handled in air at 4°C for 30 min or stored long term (>4 months) at -70°C with no observable formation of Cu(II).
17. XAS data were obtained at Stanford Synchrotron Radiation Laboratory (SSRL) beam line VII-3 as fluorescence excitation spectra with a Ge solid-state detector array. Samples (150 μl) were maintained at 10 K throughout measurements. Data reduction and analysis were performed according to standard procedures [P. J. Riggs-Gelasco, R. Mei, C. F. Yocum, J. E. Penner-Hahn, *J. Am. Chem. Soc.* **118**, 2387 (1996)]. Data were fitted with amplitude and phase functions calculated with FEFF 6.01 [J. J. Rehr *et al.*, *ibid.* **113**, 5135 (1991)], calibrated by fitting model compounds of known structure.
18. L.-S. Kau *et al.*, *ibid.* **109**, 6433 (1987).
19. D. R. Winge *et al.*, *J. Bioinorg. Chem.* **2**, 2 (1997).
20. E. I. Solomon *et al.*, *Chem. Rev.* **96**, 2563 (1996).
21. H. H. Thorp, *Inorg. Chem.* **31**, 1585 (1992).
22. I. J. Pickering *et al.*, *J. Am. Chem. Soc.* **115**, 9498 (1993).
23. D. Coucouvanis *et al.*, *Inorg. Chem.* **19**, 2993 (1980).
24. S. A. Koch *et al.*, *ibid.* **23**, 122 (1984).
25. ¹⁹⁹Hg-Atx1 was prepared by the addition of ¹⁹⁹Hg(II) to apo-Atx1 in 20 mM MES (pH 6.0). DTT was removed from apo-Atx1 by ultrafiltration before the addition of mercury. ¹⁹⁹Hg(II) (1.2 equivalents) was added to apo-Atx1 on ice with stirring. Free metal was removed with several successive washes with buffer by ultrafiltration followed by exchange into D₂O buffer. The final protein concentration was 2.40 mM with a ¹⁹⁹Hg/protein ratio of 0.83 ± 0.05 in a solution containing 25 mM sodium phosphate (pH* 6.6), 50 mM NaCl, and 98% D₂O. A similar protocol was used to prepare the EXAFS sample except that Cl⁻ was not present in any of the buffers. The final protein concentration was 3.36 mM with a Hg/protein ratio of 0.75 ± 0.06 in 20 mM MES (pH 6.0).
26. J. G. Wright *et al.*, *Prog. Inorg. Chem.* **38**, 323 (1990).
27. L. M. Utschig *et al.*, *Science* **268**, 380 (1995).
28. L. M. Utschig *et al.*, *Inorg. Chem.* **36**, 2926 (1997).
29. The ¹H(¹⁹⁹Hg) HMQC spectra of ¹⁹⁹Hg-Atx1 were obtained on a Bruker 600-MHz spectrometer (14.09 T, 107.4 MHz for ¹⁹⁹Hg) equipped with a 5-mm tunable probe. The pulse sequence and optimal delays for Met, Cys, and His ligands have been described (27). Spectral widths of 7246 Hz for ¹H (F2) and 32,221 Hz for ¹⁹⁹Hg (F1) were used. A total of 64 t₁ blocks was accumulated, with 1024 transients collected in F2 per block. The ¹H 90° pulse was 8.0 μs and the ¹⁹⁹Hg(90°)⁻¹ value was 20.4 μs, as calibrated with Hg(CH₃)₂. Safety note: The latter compound is permeable to latex gloves and is exceedingly toxic. Discussion of alternative compounds can be found at www.chem.nyu.edu/~ohallo/HgNMRStandards
30. G. R. Dieckmann *et al.*, *J. Am. Chem. Soc.* **119**, 6195 (1997).
31. J. R. R. Frausto da Silva and R. J. P. Williams, in *The Biological Chemistry of the Elements* (Clarendon, Oxford, 1991), pp. 396-397.
32. B. V. Cheesman, A. P. Arnold, D. L. Rabenstein, *J. Am. Chem. Soc.* **110**, 6359 (1988).
33. The two-hybrid analysis [L. Guarente, *Proc. Natl. Acad. Sci. U.S.A.* **90**, 1639 (1993)] was performed with the MATCHMAKER System (Clontech). Nucleotides +1 to +222 of *ATX1* were amplified by PCR and inserted at the Bam HI and Pst I sites of the pGBT9 plasmid encoding the DNA-binding domain of Gal4, to yield pPS002. For preparation of vector pPS001, CCC2 nucleotides (nt) +1 to +745 were amplified and inserted at the Eco RI and Sal I sites of pGAD424 encoding the Gal4 activation domain. The remaining three Ccc2-Gal4 fusion constructs were obtained by amplifying the corresponding CCC2 sequences and inserting them into the Bam HI and Pst I sites of pGAD424. Plasmid pCF12 contains CCC2 nt +1163 to +1582, pCF34 contains nt +1731 to +2711, and pCF56 contains nt +2831 to +3294. Yeast strain SFY526 was cotransformed with the vectors based on pGBT9 and pGAD424, and grown in 5 ml of synthetic dextrose (SD) medium to an optical density at 600 nm of 4.0. Cells were harvested, washed in water, and resuspended in 1 ml of 50 mM sodium phosphate buffer (pH 7.0) containing 10 mM KCl, 1 mM MgSO₄, and 40 mM β-mercaptoethanol. They were lysed by homogenization with glass beads after adding 45 μl of 0.1% SDS. The resulting extract (800 μl) was mixed with 200 μl of o-nitrophenyl-β-D-galactopyranoside (4 mg/ml) and incubated at 30°C overnight. After centrifugation, β-Gal activity was measured in the supernatant at 420 nm. In some instances, cells were grown in the presence of the Cu chelator BCS (3 mM). Results are representative of two to four independent samples with ranges of ≤15%. β-Gal activity units for the p53/SV40 positive controls (and vectors) were 9.75 (0.21) in the absence of BCS and 9.95 (0.27) in the presence of BCS.
34. R. P. Hausinger *et al.*, Eds., *Mechanisms of Metallo-center Assembly* (VCH, New York, 1996).
35. R. A. Steele and S. J. Opella, *Biochemistry* **36**, 6885 (1997).
36. J. Gitschier and W. Fairbrother, personal communication.
37. V. Cizewski Culotta *et al.*, *J. Biol. Chem.* **272**, 23469 (1997).
38. Supported by NIH: GM-54111 (T.V.O.), GM-38047 (J.E.P.-H.), GM-50016 (V.C.C.), Biophysics Training Grant T32GM08382 (C.P.S.), Training Grant ES 07141 (P.J.S.), and F32 DK-09305 (R.A.P.). SSRL is funded by the Department of Energy (Office of Basic Energy Sciences and Office of Health and Environmental Research) and by the NIH Biomedical Research Technology Program. The Northwestern University 600-MHz NMR Facility is funded by the W. M. Keck Foundation, NSF, NIH, and the R. H. Lurie Cancer Center. We thank R. Scott for the Cu(SC₆H₅)₃²⁻ XANES data, D. Huffman for [Cu(II)(imidazole)₄](NO₃)₂, and A. Duncan for the color illustration.

19 May 1997; accepted 4 September 1997

Measurement of the Force-Velocity Relation for Growing Microtubules

Marileen Dogterom* and Bernard Yurke

Forces generated by protein polymerization are important for various forms of cellular motility. Assembling microtubules, for instance, are believed to exert pushing forces on chromosomes during mitosis. The force that a single microtubule can generate was measured by attaching microtubules to a substrate at one end and causing them to push against a microfabricated rigid barrier at the other end. The subsequent buckling of the microtubules was analyzed to determine both the force on each microtubule end and the growth velocity. The growth velocity decreased from 1.2 micrometers per minute at zero force to 0.2 micrometer per minute at forces of 3 to 4 piconewtons. The force-velocity relation fits well to a decaying exponential, in agreement with theoretical models, but the rate of decay is faster than predicted.

It has long been speculated that the assembly and disassembly of cytoskeletal filaments, such as microtubules (MTs) and actin, can generate forces that are important for various forms of cellular motility. Examples include the motions of chromosomes

during mitosis that depend on both the assembly and disassembly of MTs (1, 2), actin-dependent motility such as cell crawling and the propulsion of *Listeria* through a host cell (3), and possibly the MT-dependent transport of intracellular membranes (4). To understand the role of force production by protein polymerization *in vivo*, it is important to determine the maximum forces that can be generated and the effect of an opposing force on the assembly dynamics of

Bell Laboratories, Lucent Technologies, 600 Mountain Avenue, Murray Hill, NJ 07974, USA.

*To whom correspondence should be addressed. Present address: F.O.M. Institute AMOLF, Kruislaan 407, 1098 SJ Amsterdam, Netherlands.